Two-electron, one-photon transitions in Cr, Fe, Co, and Cu

S. I. Salem, A. Kumar, and B. L. Scott
Department of Physics—Astronomy, California State University, Long Beach, California 90840
(Received 13 April 1983; revised manuscript received 9 December 1983)

The two emission lines resulting from the two-electron transitions $1s^{-2}\rightarrow 2s^{-1}2p_{3/2}^{-1}$, $1s^{-2}\rightarrow 2s^{-1}2p_{1/2}^{-1}$ were resolved for the transition elements Cr, Fe, Co, and Cu. Their energies were determined and were found to agree well with calculations. The relative intensities of the two transitions were measured and found to be $I(K\alpha_1\alpha_3^h)/I(K\alpha_2\alpha_3^h)\simeq\frac{3}{4}$. For the same initial state, the intensity of the emission lines resulting from the simultaneous transitions of two electrons was found to be comparable to the emission intensity from the uncorrelated single-electron transitions. This is some 3 orders of magnitude greater than what has been previously reported, both theoretically and experimentally.

I. INTRODUCTION

Correlated multielectron transitions resulting in the emission of a single photon were first predicted by Heisenberg[1] and the selection rules were formulated by Goudsmit and Gropper.[2] Their experimental detection was delayed, however, for several decades and has been reported only recently. In 1975, Wölfli *et al.*[3] observed weak emission lines in heavy ion-atom collision experiments and attributed them to the two-electron, one-photon correlated transitions. Similar experiments were later performed by Stöller *et al.*,[4] Nagel *et al.*,[5] Knudson *et al.*,[6] and Hoogkamer *et al.*[7] Nagel *et al.*[5] suggested that the observed $K^{-2}\rightarrow L^{-2}$ decay was a $2s^22p^n\rightarrow 1s^22s^22p^{n-2}$ ($E2$) transition which is parity forbidden for ($E1$) electric dipole emission. Later, however, several authors[7–10] pointed out that the energies are more accurately given by assuming an $E1$-allowed transition

$$2s^22p^n\rightarrow 1s^22s\,2p^{n-1}\,. \tag{1}$$

In these experiments, the various lines due to the multiplet splitting of the states were not resolved although the measured energies of the complex were found to be consistent with a variety of Hartree-Fock type calculations when transition (1) is assumed.

The probability that a doubly ionized atom will return to its ground state through a correlated transition (two-electron, one-photon) relative to the probability of a sequential transition giving rise to hypersatellites has been calculated by Kelly,[11] Nussbaumer,[12] Åberg *et al.*,[9] and Gavrila and Hansen.[13] Most of these calculations obtain a nonvanishing branching ratio by computing overlap integrals using different average potentials for the initial $2s$ states than for the final $1s$ states. Åberg *et al.*[9] refer to this as the "shakedown" model and found the following result:

$$B=I(K\alpha\alpha^h)/I(K\alpha^h)=(E_2/E_1)^3D_0(1s\,2s)^2\,, \tag{2}$$

where E_1 is the average hypersatellite ($K\alpha^h$) transition energy, E_2 is the average two-electron ($K\alpha\alpha^h$) transition energy, and $D_0(1s2s)$ is the $1s2s$ radial overlap integral which is approximately given by $0.187/Z$. Using this and Eq. (2) we find that the branching ratio for iron ($Z=26$) is $B\simeq 4\times 10^{-4}$. Using a similar calculation, Gavrila and Hansen[13] found $B=5\times 10^{-4}$. Kelly[11] included some correlation terms in his many-body perturbation theory calculation and found $B\simeq 1.7\times 10^{-4}$, while Nussbaumer[12] included correlations through a multiconfigurational approach obtaining results that are about 60 times smaller.

All previously measured values seem to fall between these two theoretical limits, with the exception of the experimental results recently reported by Salem *et al.*[14] These direct measurements give a branching ratio $B\simeq 0.65$ for both iron and cobalt.

II. EXPERIMENTAL PROCEDURE

The experimental approach is essentially the one traditionally used in the study of x-ray emission spectra, Fig. 1. A monoenergetic, well-collimated electron beam having an intensity of about 6×10^{16} electrons/sec impinged on a few-square-millimeter area of a clean, smooth surface of a water-cooled block of metal. The electron beam was generated by passing an electric current through a W filament attached to the high-voltage electrodes, and is

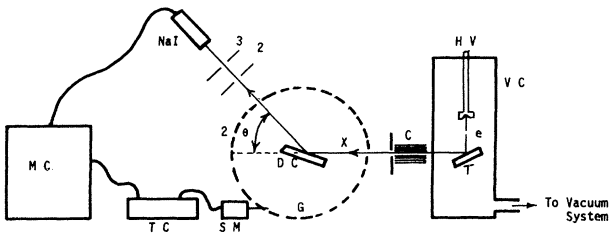

FIG. 1. Schematic diagram of experimental setup, showing from L to R, the multichannel analyzer (MC), the two-selector circuit (TC), the stepping motor (SM), the scintillation detector (NaI), the three slits (3,2,1), the diffraction crystal (DC), the high-angle goniometer (G), the x-ray beam (X), the x-ray collimator (C), the water-cooled target (T), and the electron beam (e) which is focused in a plane normal to the plane of the paper.

focused in a plane so that upon striking the target, ionization takes place along a straight line parallel to the spectrometer slits. This geometry provides maximum efficiency. The potential difference between the electron source and the target material was maintained at about 30 keV by a well-regulated power supply whose output at this load is essentially ripple free. The emission spectra were analyzed by an improved version of a single-crystal, high-angle goniometer whose resolution, at a wavelength of about 1 Å, is $\Delta\lambda/\lambda \simeq 10^{-4}$. This is a precision instrument; when lined up and calibrated for a given wavelength it maintains these properties over its entire range of operation ($5° \leq 2\theta \leq 100°$).

A calcite crystal ($2d = 6.07167$ Å) was used in the study of the spectrum of Cr, Fe, and Co, and the diffraction crystal in the case of Cu was quartz with a lattice spacing $2d = 2.7490$ Å. A time-selector circuit activated a stepping motor which changed the Bragg angle in increments of $\Delta(2\theta) = 10^{-2}$ deg and simultaneously opened the next channel on a Canberra multichannel analyzer.

The NaI crystal scintillation detector is effectively 100% efficient in detecting photons whose energy falls within the 6- to 16-keV energy range. The system was evacuated by a Vacsorb roughing pump and a fast starting triode Vacton pump, resulting in a clean vacuum of the order of 10^{-6} Torr.

The spectrometer was energy calibrated using the $K\alpha_1$ characteristic line of the element as a standard. With an electron beam intensity of 10^{16} electrons/sec, the number of counts at the peak of the $K\alpha_1$ line of a well-resolved $K\alpha_1$-$K\alpha_2$ doublet was about 10^6 counts/min. It should be noted that comparing the intensity of either the hypersatellites or the two-electron correlated transitions to that of the diagram lines is physically not significant except under identical experimental conditions,[7,15,16] as this ratio depends on the mechanism of ionization as well as the intensity and energy of the ionizing beam.

III. RESULTS

The results of this work are shown in Figs. 2—5 for Cr, Fe, Co, and Cu, respectively. The measured energies of the hypersatellites are given in Table I; the energies of the emission lines resulting from the two-electron, one-photon correlated transitions are given in Table II, and their relative intensities are listed in Table III.

In accordance with Siegbahn's scheme of designating characteristic x-ray lines, the emission line resulting from the correlated transition $1s^{-2} \rightarrow 2s^{-1}2p^{-1}$ has been designated $K\alpha\alpha^h$. Following the same general rule, the emission line resulting from the $1s^{-2} \rightarrow 2s^{-1}2p_{3/2}^{-1}$ transition is referred to as the $K\alpha_1\alpha_3^h$ line, and the one resulting from the correlated transition $1s^{-1} \rightarrow 2s^{-1}2p_{1/2}^{-1}$ is referred to as the $K\alpha_2\alpha_3^h$ (see Fig. 6).

A. Energies

The well-known energies of the $K\alpha_1$ lines of the elements[17] were taken as standards relative to which the energies of the $K\alpha_1\alpha_3^h$, $K\alpha_2\alpha_3^h$, and the energies of the hypersatellites were measured. The wavelengths of these weak lines were determined using the de Broglie condition and the angular positions of their peaks. Then their energies were readily calculated. Nonrelativistic Hartree-Fock (HF) and RHFS calculations have been used by many[8-13] to determine the energies of the correlated two-electron, one-photon transitions; in general the results are in good agreement with experimental values. The energies of these transitions may also be readily approximated from well-known quantities.

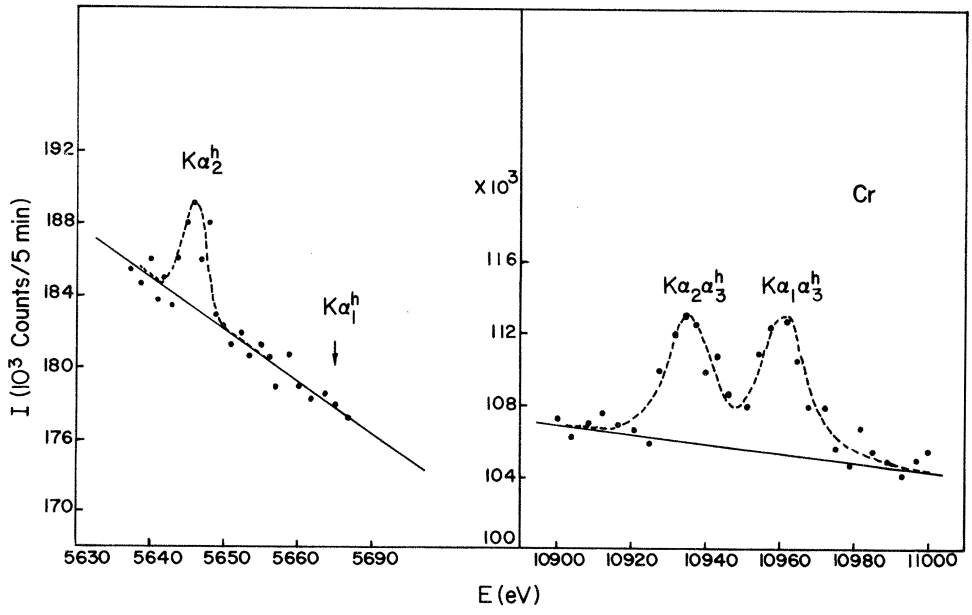

FIG. 2. Emission lines from chromium atoms having two vacancies in the $1s$ state plotted as a function of energy. (These data are not very reliable. Only one complete run was recorded before the Cr target broke. The $K\alpha_1^h$ was not observed.)

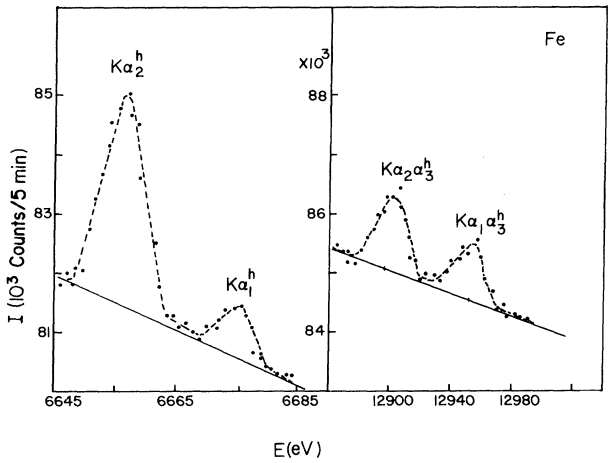

FIG. 3. Emission lines from iron atoms having two vacancies in the $1s$ state, plotted as a function of energy.

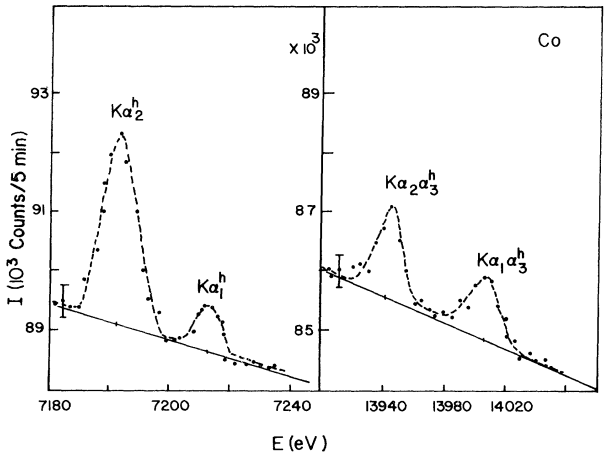

FIG. 4. Emission lines from cobalt atoms having two vacancies in the $1s$ state, plotted as a function of energy.

$$
\begin{aligned}
E(K\alpha_1\alpha_3^h) &= E(1s^{-2}) - E(2s^{-1}2p_{3/2}^{-1}) \\
&= E(1s^{-2}) - E(1s^{-1}2p_{3/2}^{-1}) \\
&\quad + E(1s^{-1}2p_{3/2}^{-1}) - E(2s^{-1}2p_{3/2}^{-1}) \\
&= E(K\alpha_1^h) + E(1s^{-1}2p_{3/2}^{-1}) - E(2s^{-1}2p_{3/2}^{-1}) \\
&\simeq E(K\alpha_1^h) + E(1s^{-1}) - E(2s^{-1}) \,. \qquad (3)
\end{aligned}
$$

Inserting the measured values of the hypersatellite energies from Table I and the values of the atomic energy levels from Bearden's tables into Eq. (3) gives the results shown in Table II for the energies of the $K\alpha_1\alpha_3^h$ line of the studied elements. The $K\alpha_2\alpha_3^h$ energies were similarly calculated and are also included in Table II.

Åberg *et al.*[9] have presented term average values of $E(K\alpha\alpha^h) - 2E(K\alpha)$ from a Hartree-Fock calculation. We have taken values from their graph ($n=6$) and combined these with the $K\alpha_1$ and $K\alpha_3$ energies to obtain the values shown in Table II. Knudson *et al.*[6] have performed similar calculations finding energies some 20—30-eV higher.

The results from Eq. (3) are generally in good agreement with the measured energies of the $K\alpha_1\alpha_3^h$ transi-

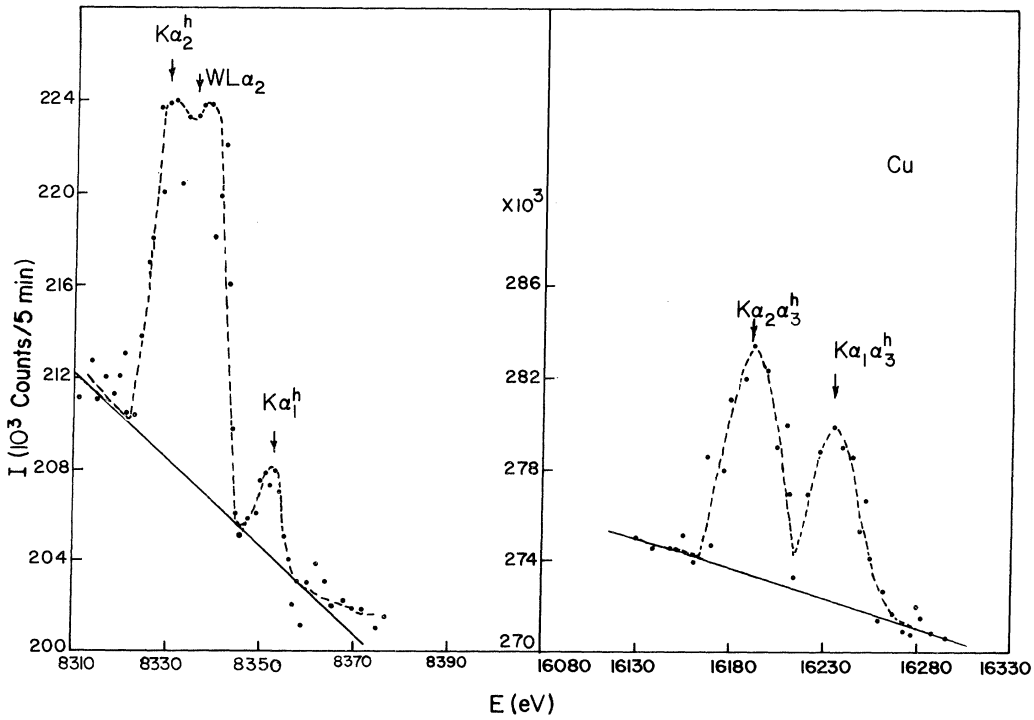

FIG. 5. Emission lines from copper atoms having two vacancies in the $1s$ state plotted as a function of energy. Also shown is the $WL\alpha_2$ line resulting from tungsten sputtered on the copper target from a heated filament.

TABLE I. The measured and calculated energies (in eV) of the $K\alpha$ hypersatellites of Cr, Fe, Co, and Cu.

Elements	Hypersatellites	Previous work	This work	Theory[a]
Cr	$K\alpha_1^h$	5666±3[b]		5664
	$K\alpha_2^h$	5650±2[b]	5645±2	5648
Fe	$K\alpha_1^h$	6679±3[b]	6675±2	6676
	$K\alpha_2^h$	6659±2[b]	6655±2	6658
Co	$K\alpha_1^h$		7207±3	7214
	$K\alpha_2^h$		7192±3	7194
Cu	$K\alpha_1^h$		8352±3	8354
	$K\alpha_2^h$	8331±3[c]	8331±3	8330

[a]Reference 19.
[b]Reference 21.
[c]Reference 20.

tions although the reason for this is not completely understood. Although only measured quantities were used with Eq. (3) in this calculation, the quantity

$$[E(1s^{-1}2p^{-1})-E(2s^{-1}2p^{-1})]-[E(1s^{-1})-E(2s^{-1})]$$

was neglected. Its value is estimated to be -50 eV so that the results calculated from Eq. (3) should be about 50 eV too large, destroying the rather fortuitous agreement displayed. Equation (3) predicts $K\alpha_2\alpha_3^h$ energies which are too large. This is probably because the only splitting accounted for is that present already in the hypersatellite level and ignores additional splitting due to the interactions with the extra $2p$ hole.

The Hartree-Fock calculations yield term-averaged energies. The splitting shown in Table II just results from the splitting of the $K\alpha$ lines to which the $K\alpha\alpha^h$ computed energies were referred. These energies are consistently somewhat higher than the measured energies.

For the studied elements, the observed energies of the correlated two-electron, one-photon transitions may be fitted by the empirical relations

$$\frac{E(K\alpha_1\alpha_3^h)}{Z(Z-2)}=20.75\pm0.01 \tag{4}$$

and

$$\frac{E(K\alpha_2\alpha_3^h)}{Z(Z-2)}=20.68\pm0.03\ . \tag{5}$$

TABLE II. The energies (in eV) of the $K\alpha_1\alpha_3^h$ and $K\alpha_2\alpha_3^h$ two-electron transitions in Cr, Fe, Co, and Cu.

		Energy in eV		
Element	Transition	From Eq. (2)	HF[a]	Observed (this work)
Cr	$K\alpha_1\alpha_3^h$	10961	10971	10962±8
	$K\alpha_2\alpha_3^h$	10940	10953	10935±8
Fe	$K\alpha_1\alpha_3^h$	12941	12961	12953±9
	$K\alpha_2\alpha_3^h$	12921	12935	12907±9
Co	$K\alpha_1\alpha_3^h$	13990	14019	14005±10
	$K\alpha_2\alpha_3^h$	13975	13989	13945±10
Cu	$K\alpha_1\alpha_3^h$	16234	16265	16236±10
	$K\alpha_2\alpha_3^h$	16213	16225	16193±10

[a]From Åberg *et al.* (Ref. 9).

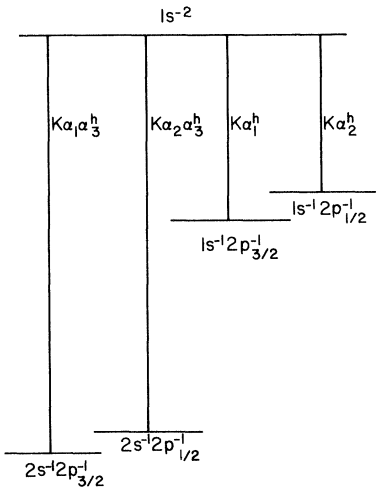

FIG. 6. Designation of emission lines from atoms with two vacancies in the $1s$ state (not to scale).

The uncertainty in Eqs. (4) and (5) is well within the errors in the measurements, but the significance of this observation is limited by the narrow range in Z covered in this experiment,[18] $24\leq Z\leq 29$.

B. Intensities

Atoms having double K-shell vacancies can deexcite by the following two different mechanisms:

(a) $1s^{-2}\rightarrow 1s^{-1}2p^{-1}$ by hypersatellite emission or
(b) $1s^{-2}\rightarrow 2s^{-1}2p^{-1}$ by two-electron, one-photon correlated transitions.

The initial states are identical ($^1S_0$) and so are the angular momentum quantum numbers of the final states. If we assume L-S coupling, the final states are ^1P and ^3P and will be split in energy by the usual Coulomb interaction. Strict L-S coupling allows only the $^1S\rightarrow{}^1P$ transition for both the hypersatellite and the correlated transitions. The experimental observation of two hypersatellite lines shows that pure L-S coupling is not achieved and some mixing occurs as would be expected. Of course, this mixing is also expected in the correlated transition.

In Table III the measured relative intensities of the hypersatellites are compared with theoretical[19] results, and the agreement is good. These results are not central to this work and have been included for comparison purposes only. The main results of this work, the correlated intensity ratios, are also presented in this table. It is interesting to note that the intensity $I(K\alpha_2\alpha_3^h)>I(K\alpha_1\alpha_3^h)$ (as is true for the hypersatellites) except for Cr where the intensities are almost equal and the experimental data is less reliable.

The two correlated transitions differ in energy by only about 50 eV for the elements investigated, so the ratio of their intensities need not be corrected for differential absorption or the reflectivity of the diffraction crystal. Thus the numerical value of this ratio should provide a rigorous test for theoretical calculations. We have been

TABLE III. Intensity ratios for single-photon emission from atoms with two K-shell vacancies. Columns marked RD contain raw data and columns marked CD have corrected data.

Element	$I(K\alpha_1^h/I(K\alpha_2^h)$ This work	$I(K\alpha_1^h/I(K\alpha_2^h)$ Theory[a]	$\frac{I(K\alpha_1\alpha_3^h)}{I(K\alpha_2\alpha_3^h)}$	$\frac{I(K\alpha_1\alpha_3^h)}{I(K\alpha_1^h)}$ CD	$\frac{I(K\alpha_1\alpha_3^h)}{I(K\alpha_1^h)}$ RD	$\frac{I(K\alpha_2\alpha_3^h)}{I(K\alpha_2^h)}$ CD	$\frac{I(K\alpha_2\alpha_3^h)}{I(K\alpha_2^h)}$ RD
Cr		0.14	1.00±0.07			0.50±0.25	1.15±0.20
Fe	0.22±0.05	0.21	0.75±0.05	0.82±0.25	1.0±0.2	0.33±0.15	0.4±0.1
Co	0.24±0.05	0.24	0.68±0.05	0.90±0.25	1.2±0.2	0.38±0.15	0.50±0.10
Cu	0.27±0.07	0.32	0.75±0.05	1.36±0.35	1.6±0.3	0.55±0.30	0.60±0.25

[a]Linearly interpolated from Ref. 19.

unable to find any calculations of this ratio in the literature, possibly because these two lines were resolved for the first time only recently.[14]

The relative intensities of the correlated transitions to the corresponding hypersatellites intensities are considerably higher than expected. They are about 3 orders of magnitude higher than previously reported experimental results as well as theoretically derived values.

The $K\alpha_1\alpha_3^h/K\alpha_1^h$ and the $K\alpha_2\alpha_3^h/K\alpha_2^h$ relative intensities are listed in Table III. The columns marked RD contain the raw data which are the observed ratio of the number of counts under the curves. The numerical values have been corrected for differential absorption in the solid target, Be window, diffraction crystal, and air path. They have also been corrected for crystal reflectivity as a function of energy and for the relative efficiency of the NaI detector.

The mass absorption coefficients of the target element at the two energies in question are close in value as they fall on opposite sides of its K absorption edge, and correction for self-absorption in the target material amounts to about only 3%.

At these energies, reflection takes place at a mean depth of about 6×10^3 atomic layers below the surface of the diffraction crystal.[22] Thus, the Bragg condition implies that the $K\alpha\alpha^h$ beam travels about twice as far as the $K\alpha^h$ beam within the crystal. As a result the effect of differential absorption in the crystal is substantially reduced. The crystal coefficients of reflectivity for the various wavelengths were obtained on the basis of the classical theory.[23]

All other corrections are straightforward, and after they were all made, the corrected results were included in the columns marked RC in Table III.

IV. DISCUSSION

The measured ratio of the correlated transition intensity to that of the hypersatellite is at variance with all previous experimental and theoretical results being some 5000 times larger. Although no clear understanding of the reasons for this large discrepancy has been found, one may present the following speculation.

In all previous experiments the desired intensity measurement was made using two distinct setups. First, a semiconductor device having a comparatively small energy resolution was used to determine the $I(K\alpha\alpha^h)/I(K\alpha)$ intensity ratio and then, in a separate experiment, the $I(K\alpha^h)/I(K\alpha)$ intensity ratio was determined using a crystal spectrometer to resolve the satellite structure. From these two values, the $I(K\alpha\alpha^h)/I(K\alpha^h)$ intensity ratio was determined. Although this procedure could have introduced some error in the final results, we do not believe it could account for the large difference involved.

A second point might be closer to the source of the discrepancy. In all previous experiments the necessary double K-shell vacancies were created using ion-atom collisions rather than the electron-atom collisions used in this work. Ion-atom collisions are generally violent, usually creating several vacancies in addition to those in the K shell. There is no theoretical reason why these additional vacancies should not occur in the $2s$ shell as well as in the $2p$ or other shells; indeed they must. An atom stripped of all $1s$ and $2s$ electrons can still emit its hypersatellite lines (although shifted to higher energies) but the correlated transition could not occur. In the extreme case in which all excited atoms had no $1s$ or $2s$ shells, and the $2s$ shells did not fill through some other mechanism, then the intensity ratio $I(K\alpha\alpha^h)/I(K\alpha^h)$ would be zero. There would be no discrepancy between the experimental results if one assumed that a large fraction of the excited atoms had empty $2s$ shells in ion-atom collisions.

The results of all ion-atom collision experiments indicate that the observed radiation is emitted by highly ionized atoms; where the correlated transitions would be immensely suppressed.

(a) The observed energies of the $K\alpha$-diagram lines are some 200-eV higher than their accepted values.[3]

(b) The observed energy of the $K\beta$-diagram line is more than 250 eV above its accepted value.[4]

(c) The observed width of the $K\beta$ line is some 500 eV,[4] while its actual width should be less than 10 eV.[24]

(d) The measured energy of the $E(K\alpha\alpha^h)$ for Fe is about 90 eV (Ref. 6) and more than 120-eV (Ref. 4) higher than the value reported in this work, and the difference seems to increase with ion energy.

Even if the above explanation of the experimental discrepancies is accepted, the large disagreement with theory remains. Most of the calculations have assumed a $2s^22p^n$ configuration for the initial state; i.e., no holes in

the $2s$ shell, as would be appropriate for the results of this experiment. Most calculations have used uncorrelated Hartree-Fock–type methods but two[11,12] have included some correlations with no significant changes. A theoretical basis for our results has not yet been found although it seems likely that electron correlations will play a large role in its explanation, much larger than that required for the corresponding absorption process.[25]

[1]W. Heisenberg, Z. Phys. 32, 841 (1925).

[2]S. Goudsmit and L. Gropper, Phys. Rev. 38, 225 (1931).

[3]W. Wölfli, Ch. Stoller, G. Bonani, M. Suter, and M. Stöckli, Phys. Rev. Lett. 35, 656 (1975).

[4]Ch. Stoller, W. Wölfli, G. Bonani, M. Stöckli, and M. Suter, Phys. Lett. 58A, 18 (1976); Phys. Rev. A 15, 990 (1977).

[5]D. J. Nagel, P. G. Burkhalter, A. R. Knudson, and K. W. Hill, Phys. Rev. Lett. 36, 164 (1976).

[6]A. R. Knudson, K. W. Hill, P. G. Burkhalter, and D. J. Nagel, Phys. Rev. Lett. 37, 679 (1976).

[7]Th. P. Hoogkamer, P. Woerlee, F. W. Saris, and M. Gavrila, J. Phys. B 9, L145 (1976).

[8]J. P. Briand, Phys. Rev. Lett. 37, 59 (1976).

[9]T. Åberg, K. A. Jamison, and P. Richard, Phys. Rev. Lett. 37, 63 (1976).

[10]W. Wölfli and H. D. Betz, Phys. Rev. Lett. 37, 61 (1976).

[11]H. P. Kelly, Phys. Rev. Lett. 37, 386 (1976).

[12]H. Nussbaumer, J. Phys. B 9, 1757 (1976).

[13]M. Gavrila and J. E. Hansen, Phys. Lett. 58A, 158 (1976).

[14]S. I. Salem, A. Kumar, B. L. Scott, and R. D. Ayers, Phys. Rev. Lett. 49, 1240 (1982); S. I. Salem, A. Kumar, and B. L. Scott, Phys. Lett. 97A, 100 (1983).

[15]Y. Isozumi, Phys. Rev. A 22, 1948 (1980).

[16]M. S. A. L. Al-Ghazi, J. Birchall, and J. S. C. McKee, Phys. Rev. A 25, 3072 (1982).

[17]J. A. Bearden, Rev. Mod. Phys. 39, 78 (1967).

[18]See Ref. 6. These authors found empirically that the energies of the unresolved $K\alpha\alpha^h$ lines could be represented by $20.0Z(Z-1)$ eV over a somewhat larger range ($12 \leq Z \leq 28$) with less than 0.5% error.

[19]M. H. Chen, B. Crasemann, and H. Mark, Phys. Rev. A 25, 391 (1982).

[20]J. P. Briand, A. Touati, M. Frilley, P. Chevallier, A. Johnson, J. R. Rosef, M. Tavernier, S. Shafroth, and M. A. Krause, J. Phys. B 9, 1055 (1976).

[21]I. Ahopelto, E. Rantavuori, and Keski-Rahkonen; Phys. Scr. 20, 71 (1979).

[22]S. I. Salem and V. H. Hall, J. Phys. F 10, 1627 (1980).

[23]A. H. Compton and S. J. Allison, *X-Ray in Theory and Experiments*, 2nd ed. (Van Nostrand, New York, 1954), p. 394.

[24]S. I. Salem and P. L. Lee, At. Data Nucl. Data Tables 18, 233 (1976).

[25]S. I. Salem, A. Kumar, K. G. Schiessel, and P. L. Lee, Phys. Rev. A 26, 3334 (1982), and references in this paper.